Supplementary Material: Arrow of Time for Continuous Quantum Measurement

In this Supplementary Material, we provide a derivation of a continuous qubit measurement that connects Eqs. (1) of the main text to the general Janus sequence construction. We also show several examples of rare and seemingly reversed qubit trajectories. Finally, we derive the distribution of $\ln\mathcal{R}$ for a qubit with no Rabi drive.

Continuous time symmetry

For the special case of two eigenvalue observables, we can construct a Janus sequence for the diffusive continuous measurement case. To see this, consider unitary dynamics followed by partial measurement collapse, such that a density operator ρ changes after a time-step δt (up to normalization) as $\rho \to M_r U \rho U^\dagger M_r^\dagger$, where U is a unitary time-evolution operator, and M_r is a measurement operator indexed by a normalized result r that we take to be a continuous variable. For a diffusive measurement to have a sensible continuum limit, it must come from a valid Gaussian POVM $E_r = M_r^\dagger M_r \propto \exp(-\delta t(r - A_h)^2/2\tau)$, where A_h is the Hermitian observable being monitored, and τ is a characteristic measurement timescale. In this limit as $\delta t \to 0$, a succession of independent Gaussian timesteps then produces a readout $r(t)$ that is a stochastic process $r(t) = \bar{A}_h(t) + \sqrt{\tau}\,\xi(t)$, where $\bar{A}_h = \mathrm{Tr}[\rho A_h]$ is the moving average of A_h.

In the same limit, the unitary dynamics may be written to first order in time δt as $U \approx 1 - i\delta t H/\hbar$, where H is the Hamiltonian. The Gaussian POVM $E_r = M_r^\dagger M_r$ naturally factors as $M_r \propto \exp(i\delta t\, r A_{ah}/2\tau - \delta t(r - A_h)^2/4\tau)$, where we include the anti-Hermitian operator iA_{ah} to allow for additional phase backaction. To first order in δt, neglecting r^2 as state-independent, this yields $M_r \propto 1 + \delta t(r/2\tau)A + \delta t A_h^2/4\tau$, where $A \equiv A_h + iA_{ah}$ contains Hermitian and anti-Hermitian parts. The r-independent term with A_h^2 is not reversible with any simple transformation of the record r; however, this term may be easily reversed by a Gaussian POVM for any observable whose square is a constant c^2 (implying A_h has eigenvalues of only $\pm c$). As such, in what follows we will assume the form $A = \boldsymbol{\alpha}\cdot\boldsymbol{\sigma}$ of an effective qubit with Pauli matrix vector $\boldsymbol{\sigma}$, so $A_h = \mathrm{Re}(\boldsymbol{\alpha})\cdot\boldsymbol{\sigma}$ and $A_{ah} = \mathrm{Im}(\boldsymbol{\alpha})\cdot\boldsymbol{\sigma}$. Similarly, we assume a general qubit Hamiltonian $H = \hbar\boldsymbol{\Omega}\cdot\boldsymbol{\sigma}/2$. These considerations then lead to a (Markovian) stochastic differential equation for the normalized qubit state ρ

$$\frac{d\rho}{dt} = \frac{1}{i\hbar}[H,\rho] + \frac{r}{\tau}\left[\frac{A\rho + \rho A^\dagger}{2} - \mathrm{Tr}\left[\frac{A + A^\dagger}{2}\rho\right]\rho\right], \quad (1)$$

expressed in the time-symmetric (Stratonovich) picture [1, 2] where $d\rho/dt \equiv \lim_{\delta t\to 0}[\rho(t+\delta t) - \rho(t-\delta t)]/2\delta t$. This equation reproduces Eqs. (1) in the main text if $\boldsymbol{\Omega} = \Omega\hat{y}$ and $\alpha = \hat{z}$.

We now examine the requirements for time-reversal symmetry of Eq. (1). The time reversed solution, $\tilde{\rho}(t) = \Theta\rho(T-t)\Theta^{-1}$, must satisfy the same equation of motion (1). Direct calculation indicates that is true, provided we transform to (time-reversed) operators, $\tilde{H} = \Theta H \Theta^{-1}$, and $\tilde{r}(t)\tilde{A} = -r(T-t)\Theta A \Theta^{-1}$. This transformation is a special case of our general Janus criterion in the main text. On physical grounds for a spin, we take the Pauli matrix vector to flip sign under time reversal, $\Theta\boldsymbol{\sigma}\Theta^{-1} = -\boldsymbol{\sigma}$, but it is straightforward to generalize this to flip the sign of only one of the Pauli matrices for a general pseudo-spin [3]. The full inversion gives the time-reversed symmetries, $\tilde{\boldsymbol{\Omega}}\cdot\tilde{\boldsymbol{\sigma}} = -\boldsymbol{\Omega}\cdot\boldsymbol{\sigma}$, and $\tilde{\boldsymbol{\alpha}}\cdot\tilde{\boldsymbol{\sigma}} = -\boldsymbol{\alpha}^*\cdot\boldsymbol{\sigma}$. We can define time reversed quantities in one of two ways. The first is an active transformation, which keeps the reference frame the same ($\tilde{\boldsymbol{\sigma}} = \boldsymbol{\sigma}$), and the second is a passive transformation, which inverts the reference frame into a left-handed system, ($\tilde{\boldsymbol{\sigma}} = -\boldsymbol{\sigma}$), thus changing the commutator structure. The active transformation (a) dictates the mappings, $\tilde{r}_a(t) = r(T-t)$, $\tilde{\boldsymbol{\Omega}}_a = -\boldsymbol{\Omega}$ (analogous to inverting an external magnetic field), and $\tilde{\boldsymbol{\alpha}}_a = -\boldsymbol{\alpha}^*$ (measuring the negated observable and reversing phase backaction), together with an inversion of the components of the Bloch coordinates, $\tilde{x}_a(t) = -x(T-t), \tilde{y}_a(t) = -y(T-t), \tilde{z}_a(t) = -z(T-t)$, which actively flips the spin. On the other hand, the passive transformation (p) inverts the sign of the measurement readout, $\tilde{r}_p(t) = -r(T-t)$, keeps the energy definitions the same $\tilde{\boldsymbol{\Omega}}_p = \boldsymbol{\Omega}$, and measures the same observable with reversed phase backaction, $\tilde{\boldsymbol{\alpha}}_p = \boldsymbol{\alpha}^*$, while preserving the coordinates in this frame, $\tilde{x}_p(t) = x(T-t), \tilde{y}_p(t) = y(T-t), \tilde{z}_p(t) = z(T-t)$. With this understanding, we can see why Eqs. (1) of the main text are invariant under the time reversal symmetry transformations discussed previously. From the passive perspective, taking $\tilde{x}(t) = x(T-t), \tilde{y}(t) = y(T-t), \tilde{z}(t) = z(T-t)$ negates the left-hand side of (1) (main text), while $\tilde{\Omega} = \Omega$, and the reversal of the readout $\tilde{r}(t) = -r(T-t)$ partially inverts the right-hand side of (1) (main text). The remaining sign reversal (effectively inverting Ω) is accounted for by the sign-flipped commutation relations of the left-handed coordinate system. From the active perspective, taking $\tilde{x}(t) = -x(T-t), \tilde{y}(t) = -y(T-t), \tilde{z}(t) = -z(T-t)$ keeps the time derivatives of (1) (main text) invariant, while $\tilde{\Omega} = -\Omega$, and $\tilde{r}(t) = r(T-t)$ keeps the right-hand side of (1) (main text) also invariant.

Examples of seemingly backward-in-time trajectories

As shown in Fig. 2 of the main text, for pure states undergoing monitored Rabi oscillations it is common to

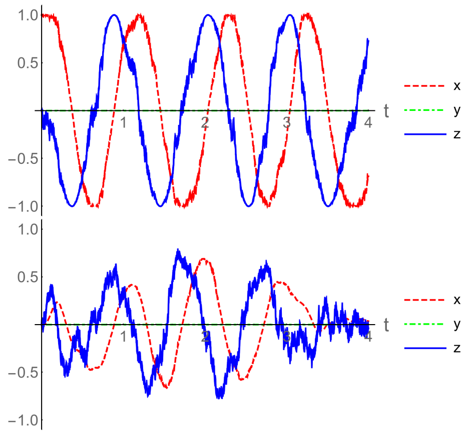

FIG. 1. Anomalous monitored Rabi oscillations with period $2\pi/\Omega = 0.5\tau$, measurement time $\tau = 2\,\mu$s, and duration $T = 2\tau$. (top) Pure initial state $x(t=0) = 1$, with a seemingly reversed log-likelihood ratio $\ln \mathcal{R} = -1.40$. Comparing to the histogram in Fig. 2(d) of the main text, such a trajectory is unlikely. (bottom) Maximally mixed initial state, with a nearly symmetric log-likelihood ratio $\ln \mathcal{R} = 5.47 \times 10^{-5}$ that is compatible with either forward or backward evolution.

observe measurement runs that appear reversed (i.e., $\ln \mathcal{R} < 0$), even for reasonably long durations T. We show an example of such a seemingly reversed trajectory in Fig. 1 (top). If we start with a completely mixed state, however, the resulting purification of the state over time due to the measurement will reveal the directionality of time, thus seemingly preventing the evolution from being time-reversed. Nevertheless, it is still possible, though unlikely, for a trajectory to erase prior purification and return to the initially mixed state. The example in Fig. 1 (bottom) shows such a time-ambiguous trajectory that begins and ends with a mixed state. This example illustrates both wavefunction uncollapse as well as time-reversal invariance with no time arrow.

Qubit with no Rabi drive

With no Rabi drive, the forward distribution of the readout $r(t)$ consisting of N independent timesteps δt for a monitored qubit with initial z-coordinate $z^i = \mathrm{Tr}(\sigma_z \rho^i)$ is $P_F(r) = \prod_{k=1}^N G_+(r_k)(1+z^i)/2 + \prod_{k=1}^N G_-(r_k)(1-z^i)/2$, where the Gaussian distributions $G_\pm(r_k)$ are centered at ± 1, respectively, with variances $\tau/\delta t$ that define the characteristic measurement time τ for obtaining a unit signal to noise ratio [4]. After a duration $T = \sum_{k=1}^N \delta t$ the integrated signal $\gamma = \sum_{k=1}^N r_k \delta t/T \to \int_0^T r(t)dt/T$ will fully determine the final qubit state. Similarly, the backwards evolution starts from the final state with z-coordinate $z^f = \mathrm{Tr}(\sigma_z \rho^f)$ and realizes the inverted measurement sequence $-r(T-t)$ with integrated signal $-\gamma$, with the distribution $P_B(-r) = \prod_{k=1}^N G_+(-r_k)(1+z^f)/2 + \prod_{k=1}^N G_-(-r_k)(1-z^f)/2$. The arrow of time estimator $\mathcal{R}$ is thus given by

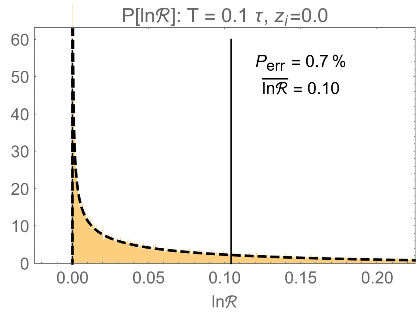

FIG. 2. Histogram of $\ln \mathcal{R}$ of 2×10^6 trajectories, with 2×10^5 bins, for qubit measurement with no Rabi drive from an initial state $x = 1$, compared to analytics (dashed). Analytically, $P_{\mathrm{err}} = 0$; the small deviation here arises from numerical error due to the finite bin size and the divergence at $\ln \mathcal{R} = 0$.

$$\mathcal{R} = \frac{P_F}{P_B} = \frac{\cosh\gamma + z^i \sinh\gamma}{\cosh\gamma - z^f \sinh\gamma}, \tag{2}$$

where z^f is related to z^i according to

$$z^f(\gamma) = \frac{z^i \cosh\gamma + \sinh\gamma}{\cosh\gamma + z^i \sinh\gamma}. \tag{3}$$

Inserting this relation into the arrow of time estimator, after some algebra, we find the result

$$\ln \mathcal{R} = 2\ln(\cosh\gamma + z^i \sinh\gamma). \tag{4}$$

We can directly find the probability distribution of $\ln \mathcal{R}$ by the relation, $P(\ln \mathcal{R}) d(\ln \mathcal{R}) = P_F(\gamma) d\gamma$. Noting the result of the derivative, $d \ln \mathcal{R}/d\gamma = 2z^f(\gamma)$, we find

$$P(\ln \mathcal{R}) = \left. \frac{P_F(\gamma)}{2|z^f(\gamma)|} \right|_{\gamma=\gamma(\ln \mathcal{R})} \tag{5}$$

with an implied sum over the two solutions of γ.

The case $z^i = 0$ is special because negative values of $\ln \mathcal{R}$ never occur. The final condition is then $z_f = \tanh\gamma$ and the solutions to the equation $x = \ln \mathcal{R} = 2\ln\cosh\gamma$ are $\gamma_\pm = \pm\cosh^{-1}(e^{x/2})$. The distribution of x thus becomes,

$$P(x) = \sqrt{\frac{\tau}{2\pi T}} \frac{e^x}{\sqrt{e^x - 1}} \exp\left\{ -\frac{T}{2\tau} - \frac{\tau}{2T}[\cosh^{-1}(e^{x/2})]^2 \right\}. \tag{6}$$

which diverges as $x^{-1/2}$ for small $x = \ln \mathcal{R}$, as shown in Fig. 2 compared to numerical simulations.

[1] E. Wong and M. Zakai, Int. J. Engng Sci. **3**, 213 (1965).
[2] B. Øksendal, *Stochastic differential equations* (Springer, Berlin, 1998).
[3] R. Winkler and U. Zülicke, Phys. Lett. A **374**, 4003 (2010).
[4] A. N. Jordan and A. N. Korotkov, Contemp. Phys. **51**, 125 (2010).